ROYAL
AERONAUTICAL
SOCIETY

REGULAR PAPER

Single channel digital controller design for a high spinning rate rolling airframe missile

E.C. Suiçmez* and A.T. Kutay

Department of Aerospace Engineering, Middle East Technical University, Ankara, Turkey
*Corresponding author. E-mail: emrecansuicmez@gmail.com

Abstract

Spinning/Rolling Airframe Missiles (RAM) mostly use an analog (ON-OFF type) control approach that deflects control surfaces (fins) at minimum and maximum positions continuously, and control is achieved by applying phase shift between the minimum and maximum deflections during a complete roll cycle. Therefore, the control signal shape changes continuously during the roll cycle. In this study, a novel single channel digital controller is designed and tested for a high spinning rate (10–20 Hz) RAM. The digital controller adjusts the amplitude of fin deflections instead of applying a phase shift. In this way, control signal shapes are predetermined in design to completely decouple yaw and pitch dynamics. At the beginning of each roll cycle, the algorithm decides on the control signal shape and amplitude to apply throughout the cycle. Delays on the actuator system and sensor measurements which might lead to instability at high spinning rates are handled effectively thanks to the predetermined control signal shapes that are changing with 90-degree intervals. Detailed geometry of a surface-to-air spinning missile is used to obtain aerodynamic coefficients for the entire flight regime (i.e. from launch to terminal phase) via Missile DATCOM. The 6-DOF flight dynamics model and the controller algorithms are built in MATLAB/Simulink environment. The proposed digital controller is tested systematically for various scenarios and the performance is compared with the conventional analog control approach. The digital controller gives better performance compared to the analog approach under the influence of servo delays and sensor noise.

Nomenclature

$C_{x_{sta}}$	body x-axes static force coefficient, negative of the DATCOM axial force coefficient C_A
$C_{y_{sta}}$	body y-axes static force coefficient, side-force coefficient
$C_{z_{sta}}$	body z-axes static force coefficient, negative of the DATCOM normal force coefficient C_N
$C_{l_{sta}}$	body axes static rolling moment coefficient
$C_{m_{sta}}$	body axes static pitching moment coefficient
$C_{n_{sta}}$	body axes static yawing moment coefficient
C_{z_q}	body z-axes force coefficient derivative with respect to the pitch rate, negative of the DATCOM coefficient C_{N_q}
C_{y_r}	side force coefficient derivative with respect to the yaw rate
C_{l_p}	rolling moment coefficient derivative with respect to the roll rate
$C_{m_{\dot{\alpha}}}$	pitching moment derivative with respect to the rate of change of angle-of-attack
C_{y_r}	Side force coefficient derivative with respect to the yaw rate
C_{m_q}	pitching moment derivative with respect to the pitch rate
C_{n_r}	yawing moment coefficient derivative with respect to the yaw rate
$V_b = [u,v,w]$	velocity components in the body fixed frame
$\omega = [p,q,r]$	body angular velocities
V_∞, a	freestream velocity and speed of sound
D,S	missile diameter (m) and reference area (m^2)

q_∞	dynamic pressure
p_n, p_e	north and east positions
h	altitude
ϕ, θ, ψ	roll, pitch, yaw angles (Euler angles)
F_a, F_p, F_g	total aerodynamic, propulsion and gravity forces
M_a	total aerodynamic moment acting on the missile center of gravity (CG)
δ	fin deflection at the controller output, actuator command
δ_{act}	fin deflection at the actuator output, actuator state
R_t	target position on Earth [North (p_n), East (p_e), Altitude (h)]
R_m	missile position on Earth [North (p_n), East (p_e), Altitude (h)]
ϕ^{360}	roll angle of the missile constrained between 0 and 360 degrees
z^{-1}	value at the previous time step
$a_{TotalCmdLimit}$	total manoeuvering g-limit of the missile
$round()$	function rounding up the value to the nearest integer
η, λ	line of sight (LOS) angles, horizontal and vertical plane respectively
α, β	angle-of-attack and sideslip angle
τ	actuator time constant
V_r	ejected mass (propellant) relative velocity in the body axes
m_0, m_f	initial and final mass of the missile
I_0, I_f	initial and final inertia tensor of the missile
T_{BE}	earth to body frame transformation matrix
K_η, K_λ	Proportional Navigation (PN) constants for the horizontal and vertical motion respectively
K_{theta}, K_{psi}	digital autopilot proportional gains

1.0 Introduction

Spinning/rolling airframe missiles have significantly different flight dynamic characteristics compared to the common roll-stabilised missiles. Dynamic instability and significant yaw/pitch coupling may occur because of the high spinning rate motion [1,2]. Control of a spinning missile can be achieved by a single actuation system with two synchronous fins. Therefore, they are smaller in size and weight, although have less manoeuverability compared to the roll-stabilised missiles [3,4]. The smaller size and weight of spinning missiles make it suitable to use as a shoulder launch platform (MANPADS) that can be serious threats for low manoeuverability aircraft (civil aircraft, cargo planes, helicopters, etc.) [5].

Because of the high spinning rates, coupling effects might lead to a divergent coning motion that makes the control system design a challenging task. Therefore, the stability and control of spinning missiles attracted many researchers. A decoupled yaw/pitch motion approach is used to design an attitude controller by Creagh and Mee [6]. Stability analysis of coning motion for a spinning missile with acceleration autopilot is given in Ref. 9, whereas similar stability analysis is performed for an attitude autopilot by Yan et al. [8]. These studies conclude that the stable region shrinks significantly if the total control system delay is above 45 degrees [7,8]. Another study focuses on the stability analysis of spinning missiles with a body-fixed (strap-down) seeker, and it shows the trade-off between guidance performance and coning motion stability considering the time-delays [2]. Cascaded three-loop autopilot with good robustness properties is designed in Ref. 3, and it is stated that sensor and actuator delays significantly contribute to the yaw/pitch couplings. Yan et al. used dynamic inverse theory to design a rate loop autopilot that compensates for the limited stability margins of spinning missiles [10].

To conclude, at higher spinning rates (above 5 Hz), the sensor and actuator delays significantly contribute to the yaw/pitch coupling so that the control problem becomes challenging [7–9, 11]. Considering this problem, the single-channel controller designed in this works aims to work on large delays and noise caused by the actuator and sensor dynamics. Most of the old spinning missiles used in the war-field use a control system that works in an analog (ON-OFF) fashion by actuating fins to the minimum or maximum positions during a complete roll cycle [4]. The analog approach achieves desired motion by applying phase shift between the minimum and maximum control signals. The analog approach highly depends on
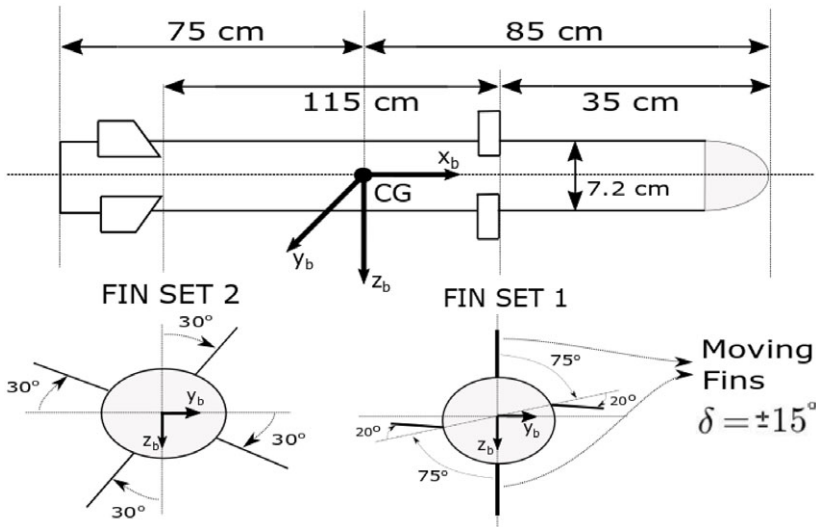
Figure 1. *Missile overview, side and back views at zero roll angle.*

roll angle measurements since applying the phase shift properly requires precise sensor measurements. Delays and noise deteriorate the performance of analog approach significantly. In this study, control authority is generated by adjusting the amplitude of fin deflections instead of applying a phase shift during the roll cycle. In this way, the control signal shapes are predetermined in the design to decouple the yaw/pitch motion effectively, and sensitivity to delays and noise are improved compared to the analog approach. The major advantage of the proposed digital control approach is better performance and robustness characteristics compared to the conventional analog approach, considering the delays and noise caused by the actuator and sensor dynamics. Systematic simulations are performed to verify the performance of the proposed controller, and to compare with the conventional analog approach. Another advantage of the proposed approach is less drag generation by the actuator system since the fins are not only actuated to a minimum or maximum position. The main disadvantage of the proposed approach is requiring a more complex actuator system, since the fins are not working in an analog (minimum/maximum) fashion. Therefore, the design and development cost of the actuator system possibly increases. To make a physically realisable control system, it is assumed that the fins can be actuated by 1-degree intervals. Although a more complex and costly actuator system is required for the proposed control approach, the performance improvement is very promising based on the simulation results.

The digital controller is mainly composed of the guidance and autopilot blocks. The autopilot block, which is the critical part of the digital controller design, tries to achieve desired angular rate commands generated by the guidance block. Details of these blocks and the algorithms are given in Section 3. The digital controller is verified using a detailed nonlinear flight dynamics model of a spinning missile that is explained in the following section.

2.0 6-DOF Flight dynamics modeling

A shoulder launched Rolling Airframe Missile (RAM) is modeled in this study. Figure 1 gives the overview of the missile including the body-fixed frame (x_b, y_b, z_b) illustration. There are two fin sets, and each set contains four fins. Fin Set-1 has two moving fins with 15 degree maximum deflection angle and two fixed fins with 20 degree dihedral angle (Fig. 1). Fin Set-2 has four fixed fins with asymmetric cross configuration. Asymmetry is common for spinning missiles since this configuration provides additional roll rate during flight. A detailed Missile DATCOM input file is generated considering the

Table 1. *Variable Mass & Inertia parameters*

Parameter	Symbol	Value	Unit
Initial mass	m_0	10	kg
Final mass	m_f	5	kg
Initial inertia matrix	I_0	diag(0.006, 1.419, 1.419)	kgm²
Final inertia matrix	I_f	diag(0.003, 1.081, 1.081)	kgm²
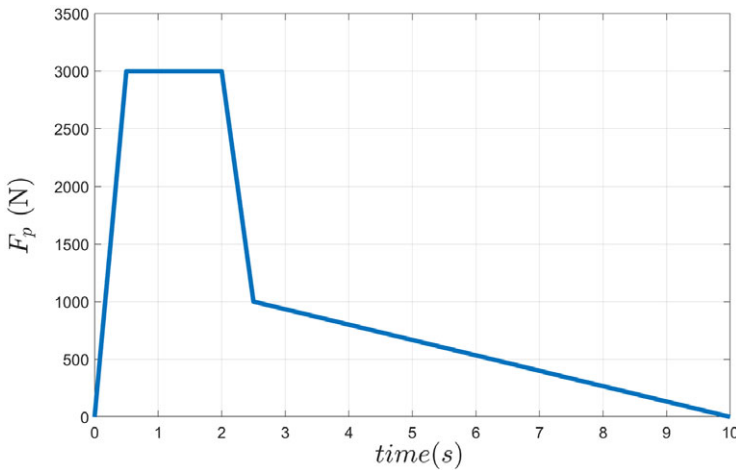
Figure 2. *Propulsion force (F_p) estimation used in the flight dynamics modeling.*

entire flight regime of the missile (see Table 2). Once the input file is generated, aerodynamic forces and moments are obtained via Missile DATCOM software [12]. Propulsion force is estimated based on the fuel mass profile and maximum flight speed that is around 2 Mach. Flight dynamics model is generated in MATLAB/Simulink environment. Equations of motion for a variable mass system are defined as follows [13].

$$\sum F = F_a + F_g = m(\dot{V}_b + \omega \times V_b) + \dot{m}V_r$$
$$-\dot{m}V_r = F_p, \quad F_a = [X, Y, Z]^T, \quad F_g = T_{BE}[0, 0, mg]^T$$
$$V_b = [u, v, w]^T, \quad \omega = [p, q, r]^T \tag{1}$$

$$\sum M = M_a = I\dot{\omega} + \omega \times I\omega + \dot{I}\omega$$
$$M_a = [L, M, N]^T$$
$$I = diag(I_{xx}, I_{yy}, I_{zz}), \quad \dot{I} = (I_0 - I_f)/(m_0 - m_f)\dot{m} \tag{2}$$

$\sum F$ and $\sum M$ are external forces applied to the center of gravity (CG) of the missile and they are represented in the body-fixed coordinate system illustrated in Fig. 1. In Equation (1), V_r is the relative velocity of ejected mass in the body axes. Therefore, the term $\dot{m}V_r$ represents the propulsion force (F_p) and can be moved to the left-hand side of the equation to be considered as an external force [13]. In Equations (1) and (2), mass and inertia values are time-dependent. Initial and final values of the mass and inertia are given in Table 1.

The following navigation and kinematic relations complete the 6-DOF equations of motion. p_n and p_e represent the north and east positions in the earth coordinate system, and h is the altitude. T_N and T_K

Table 2. *Flight conditions and actuator (fin) deflection angle used to generate the DATCOM input file*

Variable	Range
Angle-of-attack (α)	$[-30, -25, 20, \ldots, 20, 25, 30]$
Sideslip angle (β)	$[-30, 0, 30]$
Mach number	$[0.4, 0.7, 0.9, 1.1, 1.5, 2.0]$
Fin deflection angle	$[-15, 0, +15]$
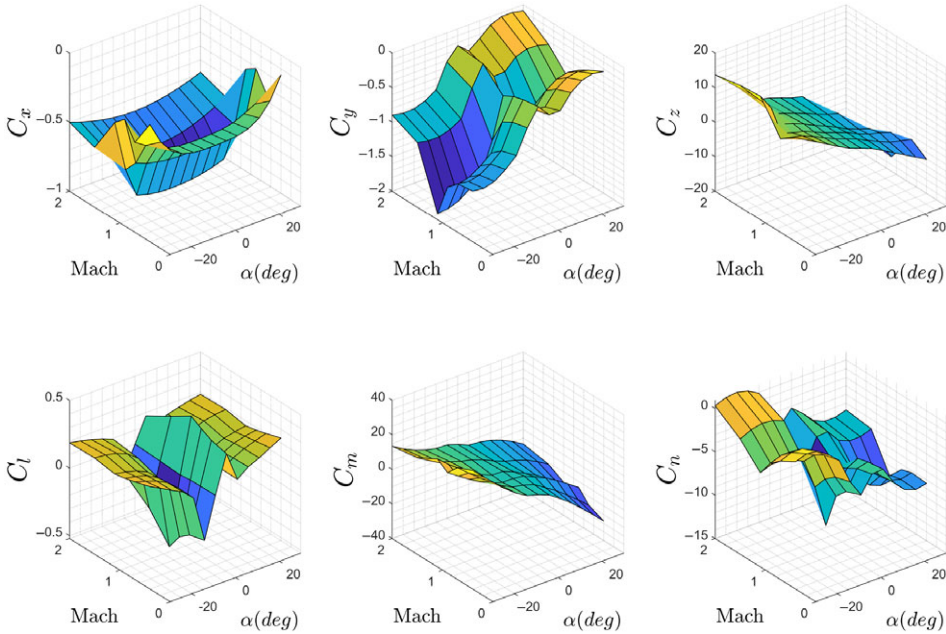
Figure 3. *Static coefficients at −15 degree fin deflection and zero sideslip and roll angle.*

are the transformation matrices [14].

$$[\dot{p}_n, \dot{p}_e, \dot{h}]^T = T_N[u, v, w]^T, \quad [\dot{\phi}, \dot{\theta}, \dot{\psi}]^T = T_K[p, q, r]^T \tag{3}$$

To estimate the propulsion force F_p for the entire flight, speed profile of the missile and drag force estimations are used. Figure 2 gives desired propulsion force with respect to time. As shown in Fig. 2, boost time is 2 seconds and the fuel is burned out at 10 seconds.

In Equations (1) and (2), aerodynamic forces and moments are estimated using the following static and dynamic coefficients that are obtained via Missile DATCOM software [11].

$$F_a = \begin{bmatrix} X \\ Y \\ Z \end{bmatrix} = \begin{bmatrix} C_x q_\infty S \\ C_y q_\infty S \\ C_z q_\infty S \end{bmatrix}, \quad M_a = \begin{bmatrix} L \\ M \\ N \end{bmatrix} = \begin{bmatrix} C_l q_\infty SD \\ C_m q_\infty SD \\ C_n q_\infty SD \end{bmatrix} \tag{4}$$
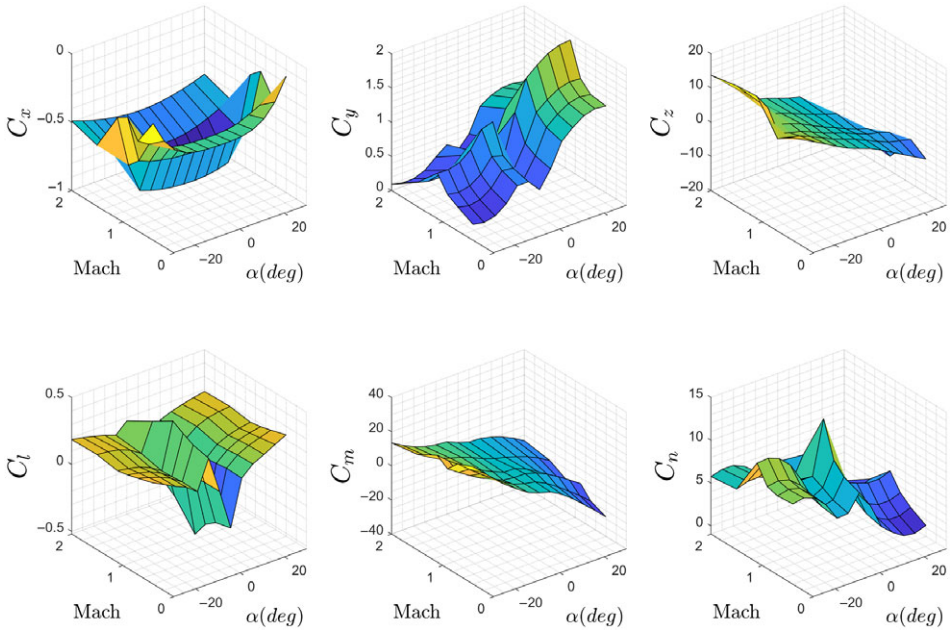
Figure 4. *Static coefficients at 15 degree fin deflection and zero sideslip and roll angle.*
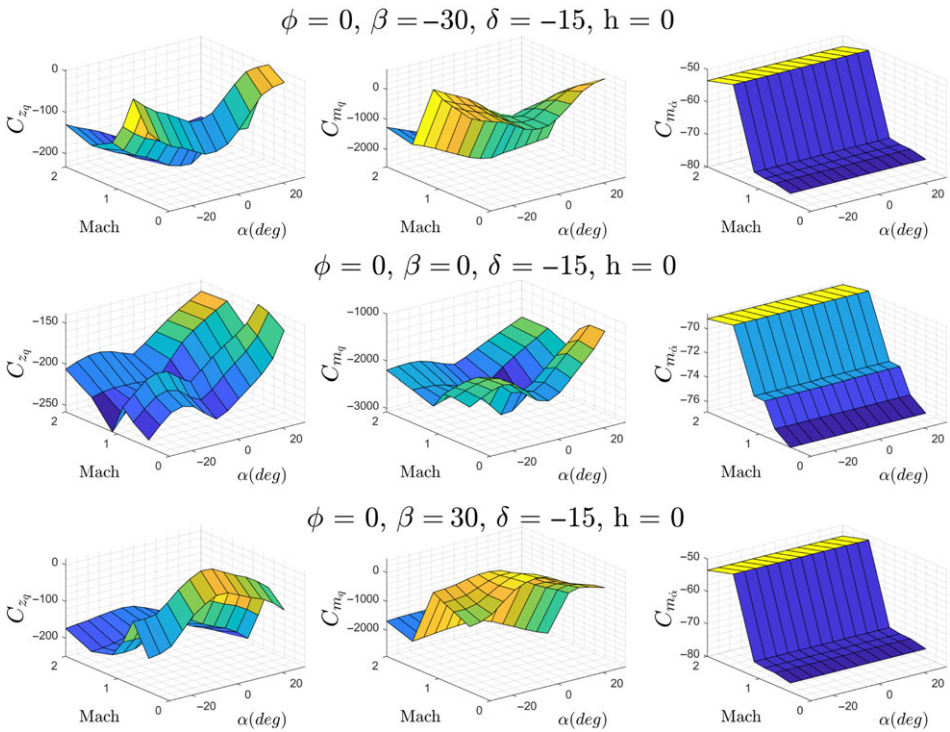
Figure 5. *Longitudinal dynamic coefficients at −15 deg fin deflection, zero roll angle and different sideslip angles.*
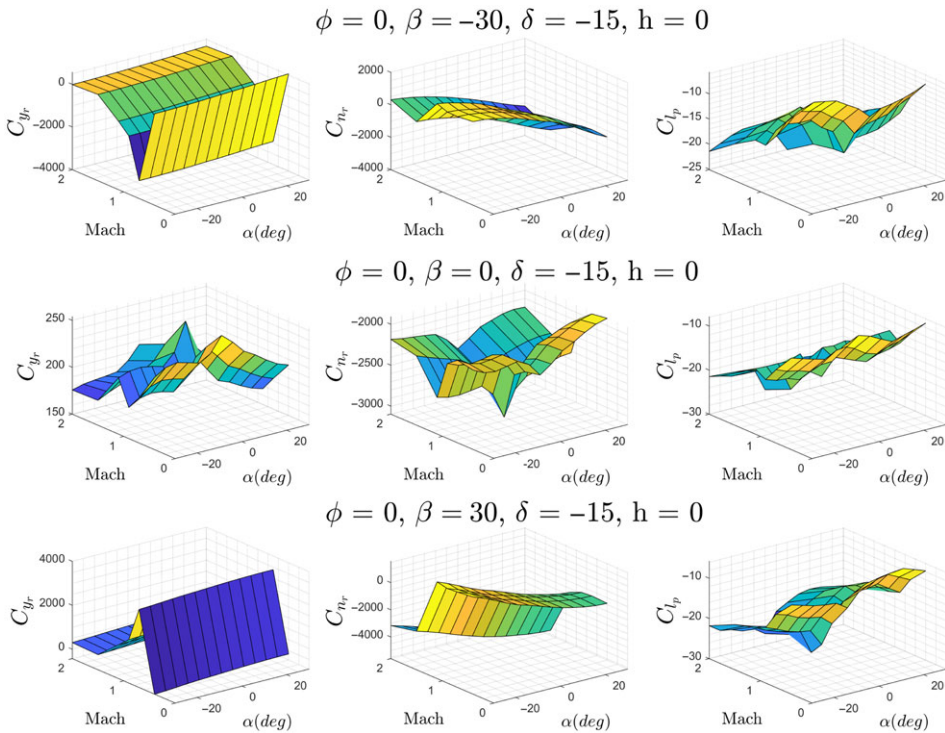
Figure 6. *Lateral dynamic coefficients at −15 deg fin deflection, zero roll angle and different sideslip angles.*

$$C_x = C_{x_{sta}}(\alpha, \beta, M, \delta)$$
$$C_y = C_{y_{sta}}(\alpha, \beta, M, \delta) + C_{y_r}(\alpha, M)\bar{r}$$
$$C_z = C_{z_{sta}}(\alpha, \beta, M, \delta) + C_{z_q}(\alpha, M)\bar{q}$$
$$C_l = C_{l_{sta}}(\alpha, \beta, M, \delta) + C_{l_p}(\alpha, \beta, M)\bar{p}$$
$$C_m = C_{m_{sta}}(\alpha, \beta, M, \delta) + C_{m_{\dot{\alpha}}}(\alpha, \beta, M)\bar{\dot{\alpha}} + C_{m_q}(\alpha, \beta, M)\bar{q}$$
$$C_n = C_{n_{sta}}(\alpha, \beta, M, \delta) + C_{n_r}(\alpha, M)\bar{r}$$
$$\bar{p} = \frac{pD}{2V_\infty} , \ \bar{q} = \frac{qD}{2V_\infty} , \ \bar{r} = \frac{rD}{2V_\infty} , \ \bar{\dot{\alpha}} = \frac{\dot{\alpha}D}{2V_\infty} \qquad (5)$$

Missile DATCOM input file is generated considering the flight regime and actuator limits of the missile given in Table 2, and also the missile geometry illustrated in Fig. 1. All the coefficients are obtained in the body-fixed coordinate system so they are independent of the roll angle. Therefore, coefficients are calculated for zero roll angle configuration given in Fig. 1.

Static coefficients at zero roll and sideslip angle are illustrated in Figs 3 and 4 for minimum and maximum fin deflection angles, respectively. Based on the results, opposite sign fin deflections (δ) at zero roll and sideslip angle cause opposite sign but approximately equal magnitude C_y and C_n coefficients, and the other static coefficients are very similar.

This is an expected result considering the movable fin orientations, which are at 0 and 180 degrees, as shown in Fig. 1. It is noted that there are sudden changes in the coefficients during the transonic region (0.8<Mach<1.2).

Longitudinal dynamic derivatives (C_{z_q}, C_{m_q}, $C_{m_{\dot{\alpha}}}$) are given in Fig. 5 for −15 degree fin deflection since dependency on the fin deflection is negligible according to the DATCOM results. Coefficients are illustrated at three different sideslip angles for Mach number and angle-of-attack sweeps. Based on the
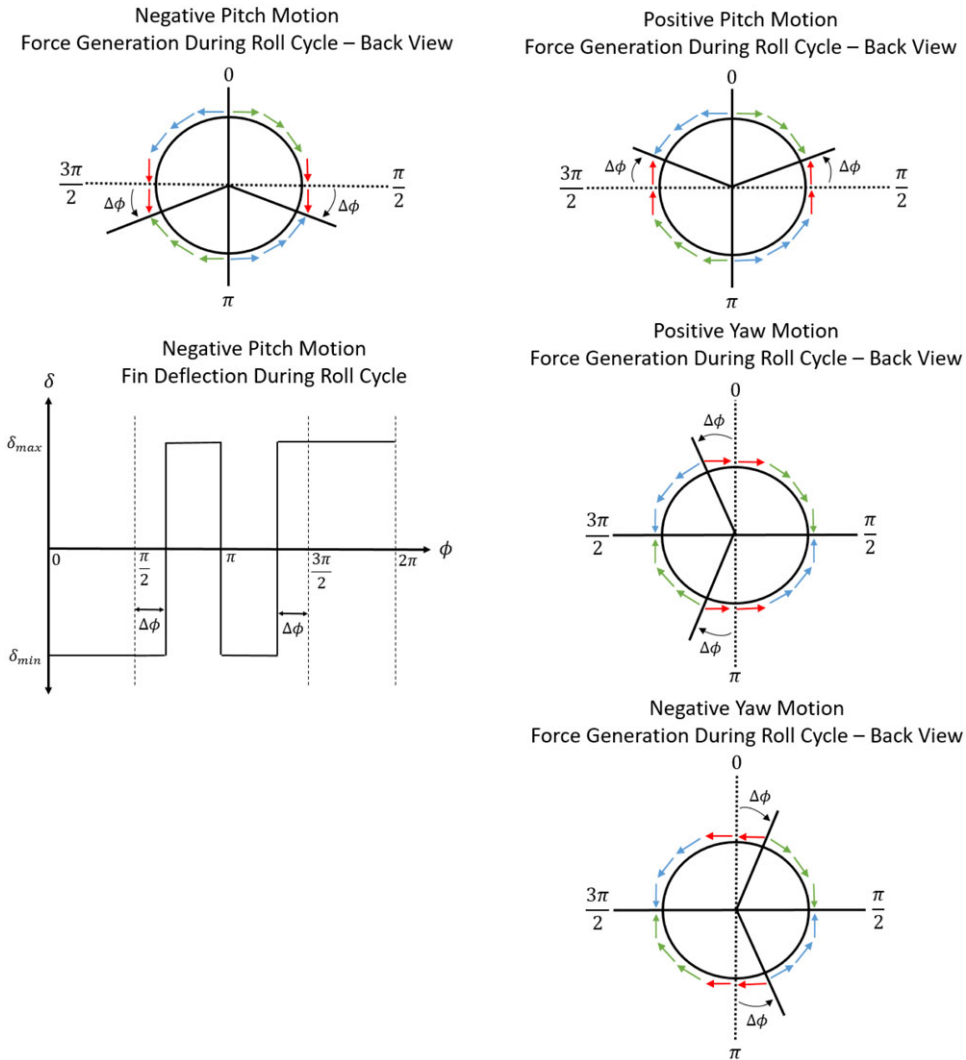
Figure 7. *Working principle of the conventional analog (ON-OFF type) controller. Force generation during a roll cycle is illustrated for each motion. Fin deflection during a roll cycle is only illustrated for negative pitch motion since the same principle is applied for other motions. Blue and green vectors represent the balanced forces, whereas the red vectors show the net force generation.*

results, C_{z_q}, C_{m_q}, $C_{m_{\dot{\alpha}}}$ mainly changes with respect to the Mach number. Smaller variations are observed with respect to the angle-of-attack according to Fig. 5.

Similar to the longitudinal motion, DATCOM results of lateral dynamic derivatives (C_{y_r}, C_{n_r}, C_{L_p}) are also independent of the fin deflection (δ), and mainly change with respect to the Mach number. Coefficients are illustrated at -15 degree fin deflection and three different sideslip angles. According to Fig. 6, C_{y_r} and C_{n_r} results are not reasonable at high sideslip angles (-30 and 30). Therefore, C_{y_r} and C_{n_r} coefficients are used for zero sideslip angle, and they are functions of the angle-of-attack and Mach number only as shown in Equation (5). C_{L_p} values are reasonable for three different sideslip angles, and it is formulated as a function of the angle-of-attack, sideslip angle and Mach number.
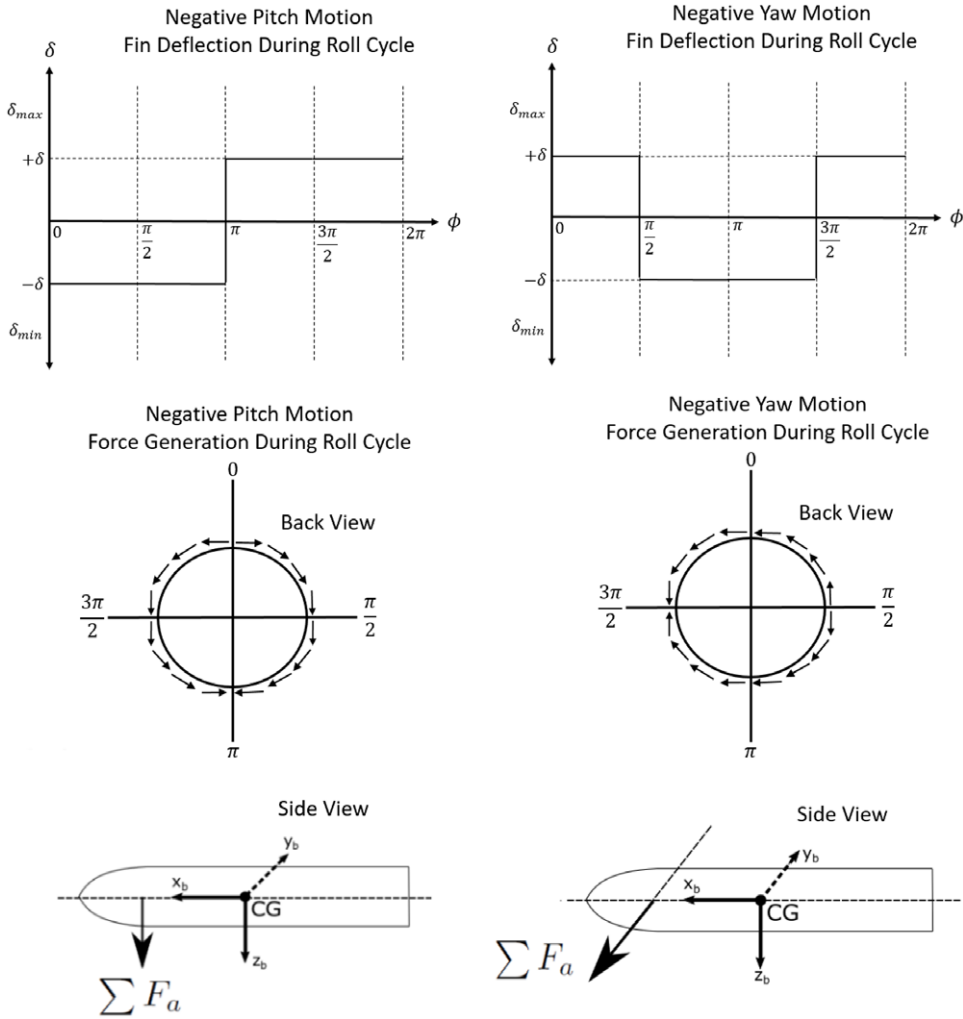
Figure 8. *Working principle of the proposed digital control approach. Only the negative motion is illustrated since the principle is the same for positive motion (i.e. opposite fin deflections are applied for positive motions).*
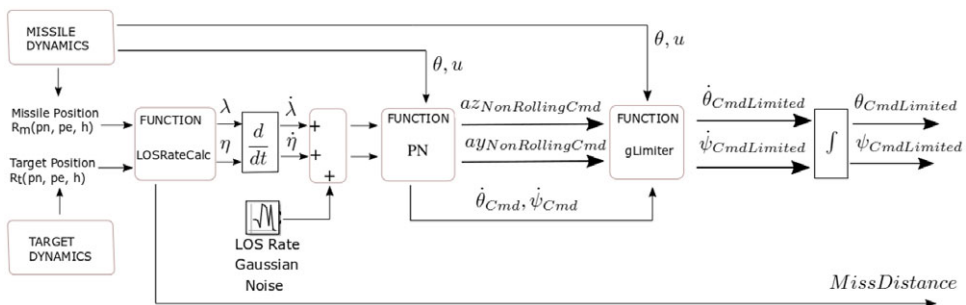
Figure 9. *The guidance block diagram.*

Table 3. *Guidance block functions*

---

function $[\eta, \lambda, MissDistance] = $ **LOSRateCalc**(R_m, R_t)

$\lambda = atan2((R_t(3) - R_m(3)) , \; sqrt((R_t(1) - R_m(1))^2 + (R_t(2) - R_m(2))^2))$

$\eta = atan2(R_t(2) - R_m(2) , \; R_t(1) - R_m(1))$

$MissDistance = sqrt((R_t(1) - R_m(1))^2 + (R_t(2) - R_m(2))^2 + (R_t(3) - R_m(3))^2)$

---

function $[az_{NonRollingCmd}, ay_{NonRollingCmd}, \dot{\theta}_{Cmd}, \dot{\psi}_{Cmd}] = $ **PN**$(\lambda, \eta, \theta, u)$

$\dot{\theta}_{Cmd} = \lambda \, K_\lambda$

$\dot{\psi}_{Cmd} = \eta \, K_\eta$

$q_{NonRollingCmd} = \dot{\theta}_{Cmd}$

$r_{NonRollingCmd} = cos(\theta) \, \dot{\psi}_{Cmd}$

$az_{NonRollingCmd} = -q_{NonRollingCmd} \, u$

$ay_{NonRollingCmd} = r_{NonRollingCmd} \, u$

---

function $[\dot{\theta}_{CmdLimited}, \dot{\psi}_{CmdLimited}] = $
gLimiter$(g_{Limit}, az_{NonRollingCmd}, ay_{NonRollingCmd}, \dot{\theta}_{Cmd}, \dot{\psi}_{Cmd}, \theta, u)$

$g = 9.81$

$a_{TotalCmd} = sqrt(az^2_{NonRollingCmd} + ay^2_{NonRollingCmd})$

$a_{TotalCmdLimit} = g_{Limit} \, g$

if $a_{TotalCmd} > a_{TotalCmdLimit}$

$\quad az_{NonRollingCmdLimited} = az_{NonRollingCmd} \, sqrt(a^2_{TotalCmdLimit}/a^2_{TotalCmd})$

$\quad ay_{NonRollingCmdLimited} = ay_{NonRollingCmd} \, sqrt(a^2_{TotalCmdLimit}/a^2_{TotalCmd})$

$\quad \dot{\theta}_{CmdLimited} = -az_{NonRollingCmdLimited}/u$

$\quad \dot{\psi}_{CmdLimited} = ay_{NonRollingCmdLimited}/(u \, cos(\theta))$

else

$\quad \dot{\theta}_{CmdLimited} = \dot{\theta}_{Cmd}$

$\quad \dot{\psi}_{CmdLimited} = \dot{\psi}_{Cmd}$

end
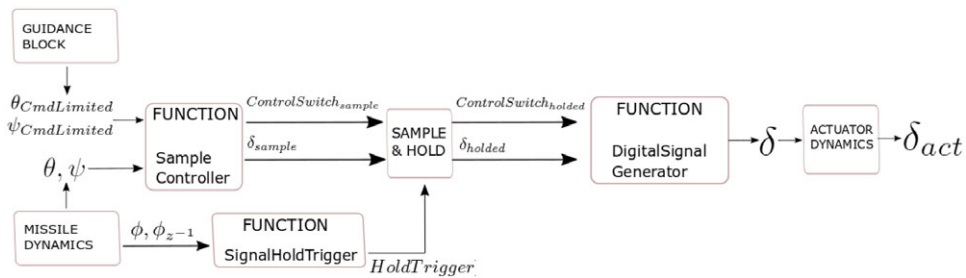
Figure 10. *The digital autopilot block.*

Aerodynamic and propulsion models are generated in this section to build the 6-DOF flight dynamics model of the spinning missile. In the next section, single-channel digital autopilot design is given in details.

3.0 Single-channel digital autopilot design

Old type spinning missiles are generally controlled via an analog (ON-OFF type) control approach [4]. Symmetric fins can only be actuated to the minimum or maximum deflections. Missile is controlled by

Table 4. *Autopilot block functions*

---

function $[ControlSwitch_{sample}, \delta_{sample}] = \textbf{SampleController}(\theta_{CmdLimited}, \psi_{CmdLimited}, \theta, \psi)$
$e_{\theta} = (\theta_{CmdLimited} - \theta)\,180/pi$
$e_{\psi} = (\psi_{CmdLimited} - \psi)\,180/pi$
$\delta_{\theta} = e_{\theta} \cdot K_{theta}$
$\delta_{\psi} = e_{\psi} \cdot K_{psi}$
if $abs(e_{\theta}) - abs(e_{\psi})$
   $ControlSwitch_{sample} = 0$
    $\delta_{sample} = \delta_{\theta}$
else
   $ControlSwitch_{sample} = 1$
    $\delta_{sample} = \delta_{\psi}$
end
$\delta_{sample} = round(\delta_{sample})$

---

function $[HoldTrigger] = \textbf{SignalHoldTrigger}(\phi, \phi_{z^{-1}})$
$\phi^{360} = mod(\phi\,180/pi, 360)$
$\phi_{z^{-1}}^{360} = mod(\phi_{z^{-1}}\,180/pi, 360)$
if $\phi^{360} - \phi_{z^{-1}}^{360} > 0$
   $HoldTrigger = 0$
else
   $HoldTrigger = 1$
end

---

function $[\delta] = \textbf{DigitalSignalGenerator}(ControlSwitch_{holded}, \delta_{holded}, \phi^{360})$
switch $ControlSwitch_{holded}$
     case 0
       if $(\phi^{360} > 0$ & $\phi^{360} < 180)$
       $\delta = -\delta_{holded}$
       else
       $\delta = \delta_{holded}$
       end
     case 1
       if $(\phi^{360} > 90$ & $\phi^{360} < 270)$
       $\delta = -\delta_{holded}$
       else
       $\delta = \delta_{holded}$
       end
     end

---

applying phase shift between the minimum and maximum fin deflections during the roll cycle. The working principle of the analog type control approach is illustrated in Fig. 7. Left side of the figure shows the force generation and fin deflection plots during a roll cycle to generate a negative pitch motion. Similarly, the right side shows the generation of desired forces for each motion, but fin deflection plots are not illustrated since the working principle is the same. Switching between the minimum and maximum fin deflections is shifted by $\Delta\phi$ to generate the desired force. Note that, in the balanced condition (i.e. zero net force generation), minimum and maximum fin deflection change with 90 degree interval in roll angle. $\Delta\phi$ is proportional to the normalised error, and maximum 45 degree phase shift is allowed. Maximum phase shift value and the proportional gain are tuned using the nonlinear simulations. In Fig. 7, blue and green color vectors cancel out for each case, and the net force generation is represented
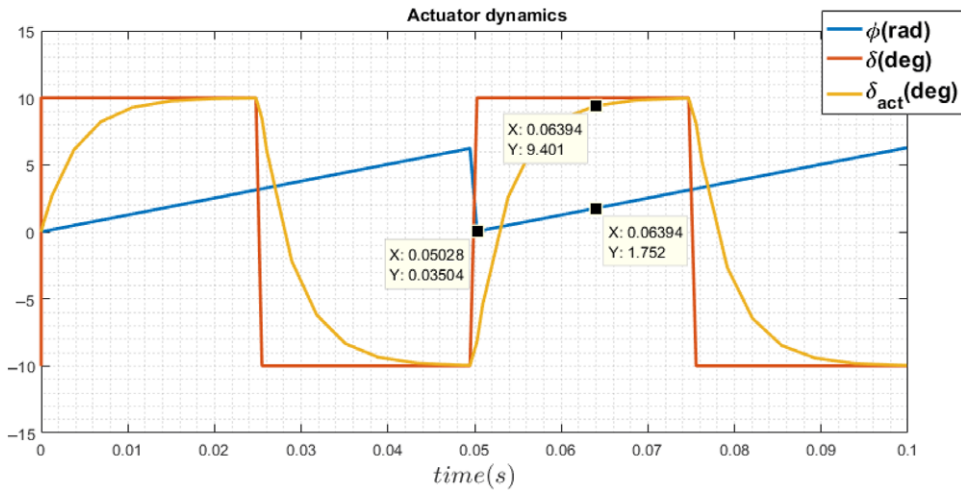
Figure 11. *Actuator response with respect to roll angle at 20 Hz spinning rate.*

by the red color vectors. This approach requires on-off type simple actuator systems that is advantageous considering the cost and simplicity. However, the analog approach is highly sensitive to the delays and noise since high precision roll angle measurement is required to apply the phase shift properly. Considering that the maximum phase shift ($\Delta\phi_{\max}$) is 45 degrees, even small delays might lead to undesired motions.

Moreover, it is hard to decouple yaw and pitch dynamics for the analog approach in case of delays or unmodeled dynamics, since the control signal shape is changing continuously during the roll cycle. Strong yaw/pitch coupling of spinning missiles, and its negative effect on stability and performance are emphasised in the literature [7,8]. To resolve these problems, predefined control signal shapes are applied during a complete roll cycle instead of applying a continuously changing control signal shape via phase shift. Predefined control signal shapes are determined based on the decoupled pitch and yaw motion. The proposed approach achieves control by adjusting the amplitude of fin deflections instead of applying only the minimum and maximum fin deflections. Therefore, it requires variable fin deflections that require more complex actuator system compared to the analog type (ON-OFF) actuators. Although the complexity and cost of the actuator system increases, the performance and robustness properties are improved significantly compared to the conventional analog control approach. Simulation results show the performance improvement for various test cases. The proposed novel control approach is referred as "digital control approach" throughout the paper, and the detailed design is explained in the following paragraphs.

First, the yaw and pitch dynamics are decoupled and predefined control signal shapes are determined. Figure 8 shows the control signal shapes to generate negative pitch and yaw motion. Similarly, positive pitch and yaw motions are achieved by applying the opposite direction control signal shapes which are not illustrated in Fig. 8. As shown in the back views, net forces are generated in the desired direction only. In other words, the yaw and pitch motions are totally decoupled. Compared to the analog approach, control signal shapes are fixed for each motion, but amplitude of fin deflections change based on the error. At the beginning of each roll cycle, the controller decides on the predetermined control signal shape to achieve the desired motion. Desired motion refers to the motion with highest priority (i.e. the largest error). Then, magnitude of the fin deflection is determined proportional to the error. Therefore, the method requires variable fin actuator systems instead of analog type ON-OFF actuators. It is assumed that the actuator system can rotate the fins with 1 degree interval between the minimum and maximum fin deflection (i.e. ±15 degrees). The digital control approach still depends on roll angle measurement to switch between the positive and negative fin deflections. However, switching occurs at fixed 90 degree intervals (see Fig. 8). The main driver for the digital controller is adjusting the fin deflection amplitude
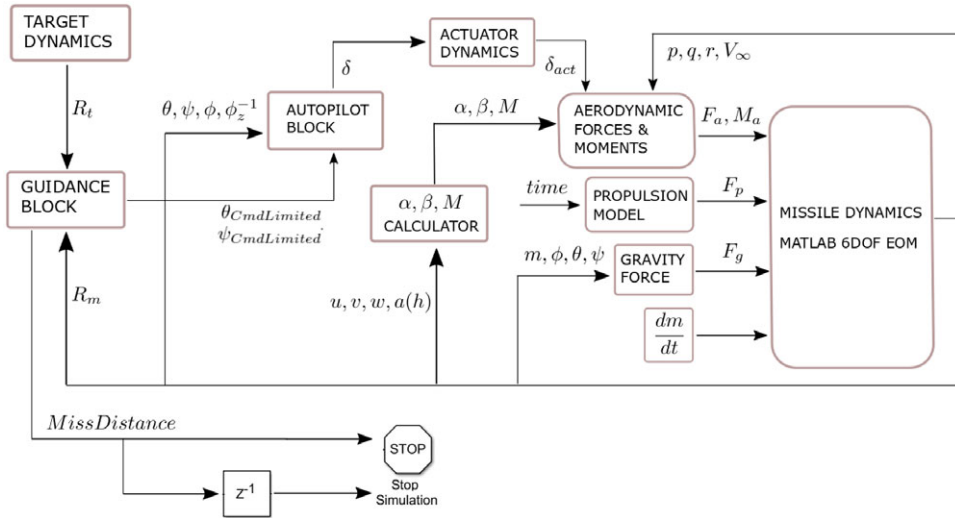
Figure 12. *Overview of the main simulation block build in MATLAB/Simulink.*

based on the error dynamics. Therefore, the digital control approach is more robust against the delays in measurement or actuator systems compared to the conventional analog control method described previously. A general explanation of the digital controller is given in this paragraph. Details of the implementation will be given throughout this section via algorithms and block diagrams.

The digital controller is composed of two main blocks, named as guidance and autopilot. The autopilot requires Euler angle commands that are generated by the guidance block. The guidance block and its functions are given in Fig. 9 and Table 3, respectively. Guidance algorithm first calculates the Line-Of-Sight (LOS) angle rates ($\dot{\eta}, \dot{\lambda}$) using the missile and target positions with respect to the Earth-fixed NED (North-East-Down) frame [3]. Gaussian distributed noise (with mean=0 and variance=1) is added to the LOS rate calculations to simulate the measurement noise. Proportional Navigation (PN) guidance law is used to calculate acceleration commands in the non-rolling body-fixed frame. PN law constants (K_λ, K_η) are chosen as 3 for the vertical and horizontal motion based on the general implementation in literature [3]. Finally, desired acceleration commands are limited considering the total g-limit of the missile, and transformation from acceleration commands to Euler angle commands ($\theta_{CmdLimited}, \psi_{CmdLimited}$) is performed. g-limit of the missile is taken as 10g considering the similar short-range spinning missiles [3,15].

Once the Euler angle commands are generated by the guidance block, they are sent to the digital autopilot block. The autopilot block and its functions are given in Fig. 10 and Table 4, respectively. At the beginning of each roll cycle, the autopilot compares the error in both channels and adjusts the actuator signal shape to control the channel with larger error (see Fig. 8). In other words, the autopilot prioritises the channel with larger error, and predetermined control signal shape is applied during that roll cycle. For a complete roll cycle, the net force generated by the actuators works totally to decrease the error on the prioritised channel. Therefore, the autopilot generates actuator signals to decouple the pitch and yaw dynamics completely. Amplitude of the actuator signal is determined by multiplying the error with proportional gains K_{theta} and K_{psi} (Table 4, SampleController). Proportional gains are constant for the entire flight and tuned to the value of 4 using the nonlinear simulations. To generate the control signal shapes as illustrated in Fig. 8, a sample holder block with SignalHoldTrigger function (Table 4) is used to hold the actuator signals during the roll cycle. As shown in Table 4, if $ControlSwitch_{holded}$ is zero, the autopilot generates a signal shape to control the pitch motion; otherwise, if $ControlSwitch_{holded}$ is one, then the signal shape generated by the autopilot aims to control the yaw motion. As mentioned previously, it is assumed that the actuators can rotate the fins with 1 degree interval between −15 and
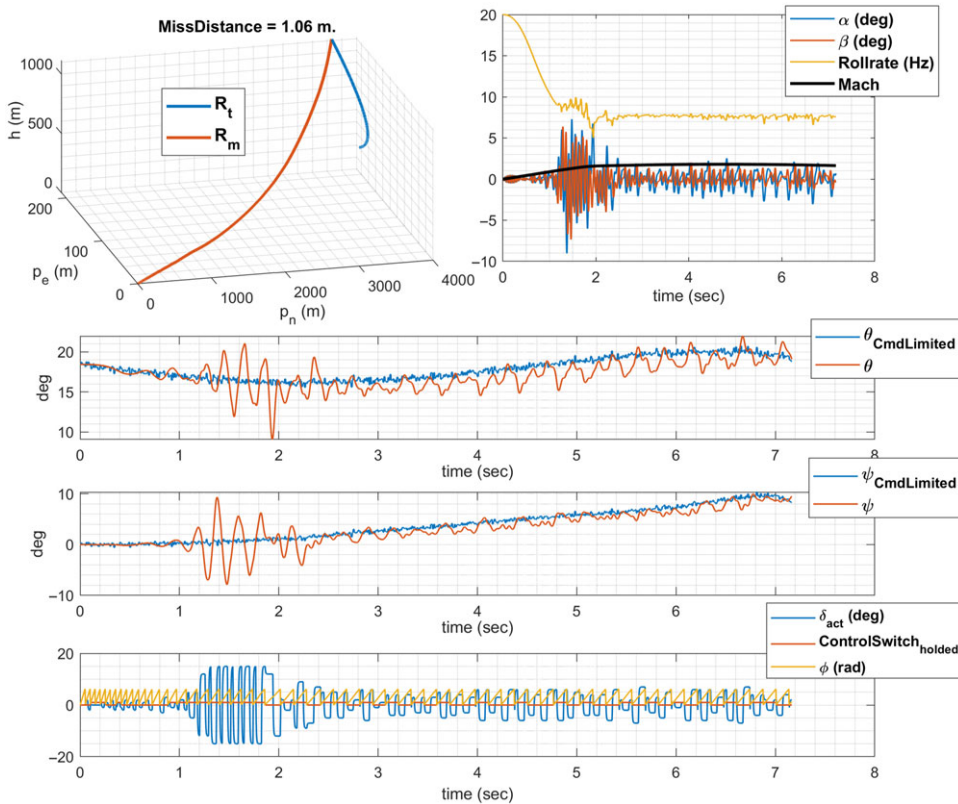
Figure 13. *The digital controller simulation results for 100 m/s target speed with 1 g target manoeuver.*

+15 degrees. Therefore, the autopilot generates actuator commands with 1 degree interval. "round" function is added at the end of the SampleController function (Table 4) for this purpose. Once the actuator signal (δ) is generated by the autopilot, it is delayed by the actuator dynamics block described in the next paragraph.

Actuator dynamics is modeled as a first order system with time constant of 0.005 seconds considering the similar studies about spinning missiles [9].

$$\delta_{act} = \frac{\delta}{\tau s + 1}, \quad with \ \tau = 0.005 \text{sec.} \tag{6}$$

For our case, the missile has approximately 20 Hz maximum spinning rate. At this rate, the actuator response with respect to the roll angle is given in Fig. 11, and it can be seen that fin deflection reach %95 of the desired input after approximately 90 degree phase lag in roll angle. According to Fig. 8, fin deflections change with 90 degree intervals. Therefore, actuator dynamics introduce a significant delay to the system. However, the large delay does not effect the controller considerably since the digital autopilot does not require very precise roll angle measurements which is one of the main advantages of the proposed controller.

The proposed digital control approach is described in this section. In the next section, the digital controller is tested via nonlinear simulations. Overview of the simulation block is illustrated in Fig. 12. Systematic simulations are performed to compare the digital controller with the conventional analog controller. To simulate the analog control approach, only the autopilot block given in Fig. 12 is replaced with the analog autopilot that is described in Fig. 7.
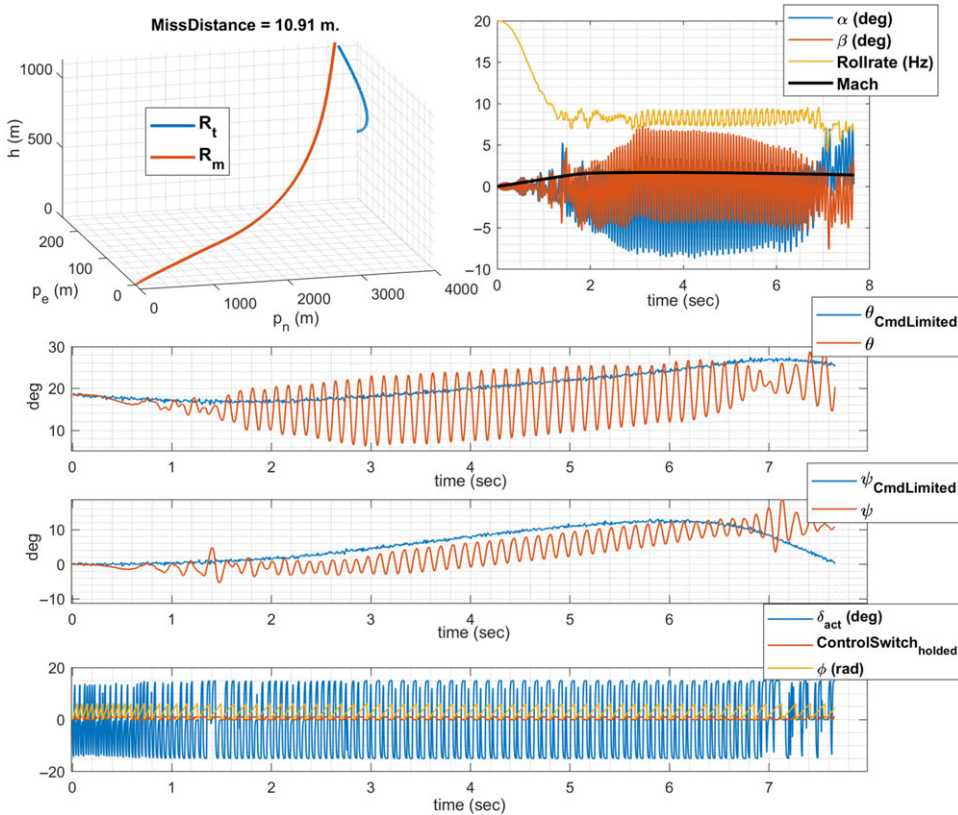
***Figure 14.** The analog controller simulation results for 100 m/s target speed with 1 g target manoeuver.*

4.0 Simulation results

The simulation block illustrated in Fig. 12 is generated using MATLAB/Simulink environment. Simulations run at 400 Hz considering the 20 Hz maximum spinning rate. Missile dynamics is simulated using the total forces and moments formulated in Equations (1) and (2). Aerodynamic forces and moments are calculated via 4D (α, β, M, δ) look-up tables. All the forces and moments are represented in the body-fixed frame. Target dynamics is included considering a fixed-point mass and basic kinematic relations. Distance between the target and missile (i.e. the "Miss Distance") is used to end simulations. Simulations are performed for 15 seconds considering the approximate flight duration of a shoulder launched spinning missile, and propulsion force shown in Fig. 2.

Simulations are performed systematically considering different target dynamics. Target speed varies between 100 and 300 m/s with 50 m/s intervals. Target acceleration is chosen as 1, 2 and 3 g. Acceleration refers to the total acceleration in the lateral and vertical motion. For each speed and acceleration, three different manoeuvers are tested. To conclude, a total of 54 cases are tested. It is noted that the maximum target acceleration is chosen as 3 g considering the fact that in general, a missile needs to have three times target manoeuverability to hit the target [3].

Since there are 54 cases, results are illustrated in details only for one case for both the digital and analog approach. For the other cases, mean and standard deviation of the error and miss distance are given for the digital control approach. In addition, the digital and analog approaches are compared. However, the comparison is made for only 1 and 2 g acceleration target manoeuvers at low target speeds (i.e. 100 and 150 m/s) since the analog approach's performance is not satisfactory at high speed and manoeuvering targets.
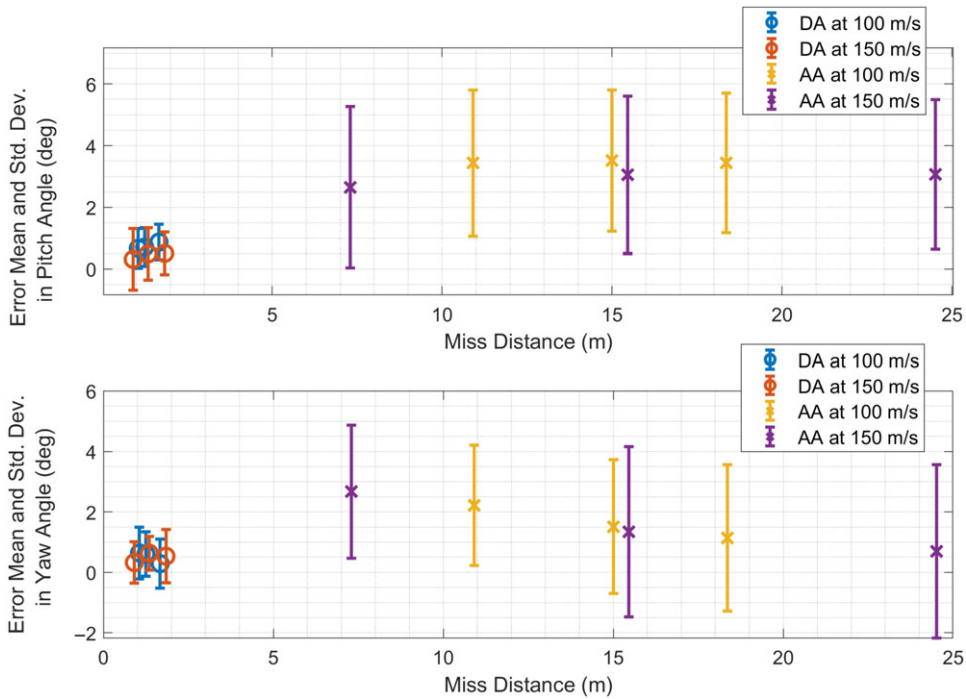
Figure 15. *Performance comparison between the digital autopilot (DA) and analog autopilot (AA) at low speed 1 g target manoeuvers.*

First, the digital and analog approaches are tested at 100 m/s target speed with 1 g manoeuver. Results are illustrated in Figs 13 and 14 for the digital and analog controller, respectively. The analog approach deflects fins to the minimum and maximum values (i.e. ± 15 degrees), and the control is achieved by applying phase shift between the minimum and maximum deflections (see Fig. 7). With increasing time, the analog approach results in highly oscillatory motion, which is not desired. Results of the digital controller is much less oscillatory since fin deflection is adjusted based on the error, and the control signal shapes are decoupled and predetermined in the design (see Fig. 8). Actuator system and measurement delays and noise are more disruptive for the analog controller compared to the digital controller. This is an expected result since the digital controller has predefined control signal shapes, and switching between the positive and negative fin deflections occurs with fixed 90 degree intervals (see Fig. 8).

The digital and analog controller are tested at 54 cases mentioned previously, and it is observed that the analog controller can only work against targets with low speed and manoeuverability. Figures 15 and 16 show the comparison results at 1 and 2 g target manoeuvers with 100 and 150 m/s target speeds. The analog controller has higher error magnitudes compared to the digital controller, and miss distances are not acceptable for some cases.

The digital controller's performance is given in Figs 17, 18, 19 for 1, 2 and 3 g target manoeuvers with different target speeds in terms of miss distance and error magnitudes. It is observed that the overall performance is satisfactory. The miss distance and error are slightly larger for higher target acceleration.

To conclude, the proposed digital control approach has satisfactory performance for most of the test cases considering the actuator delays, sensor noise and strong couplings caused by the high spinning rates. On the other hand, the conventional analog control approach does not give desired performance, and only works at low target manoeuvers and speed.
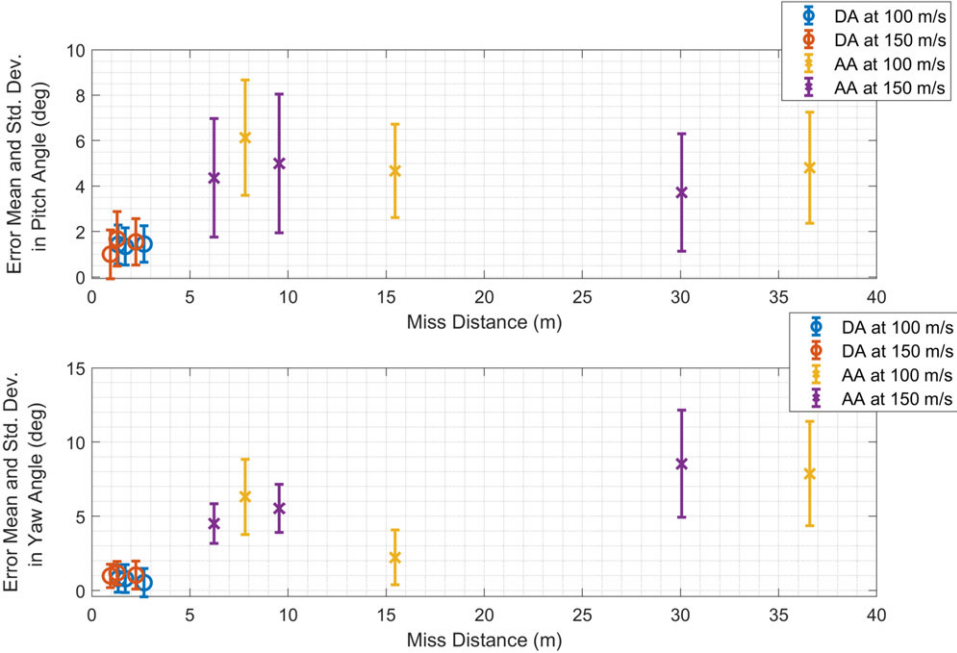
Figure 16. *Performance comparison between the digital autopilot (DA) and analog autopilot (AA) at low speed 2 g target manoeuvers.*
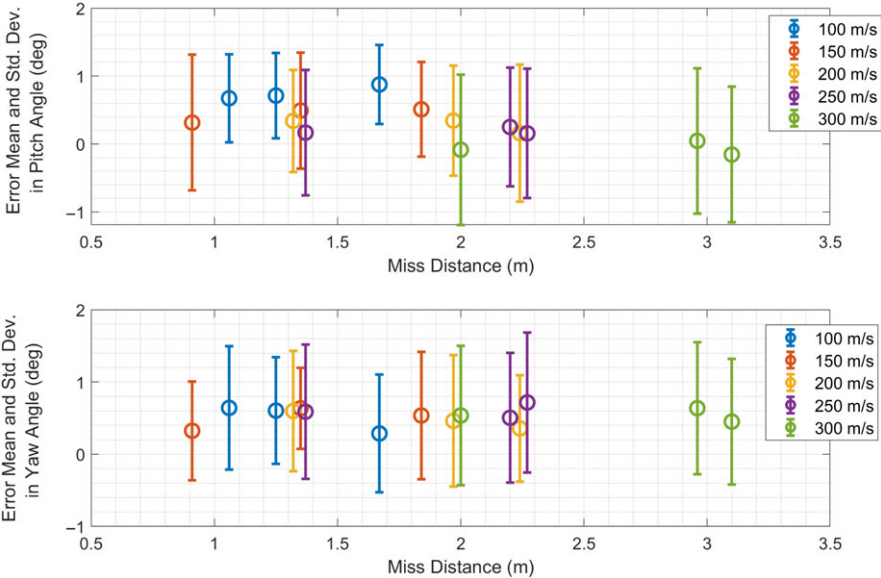
Figure 17. *The digital autopilot performance results for target manoeuvering at 1 g with different target speeds.*
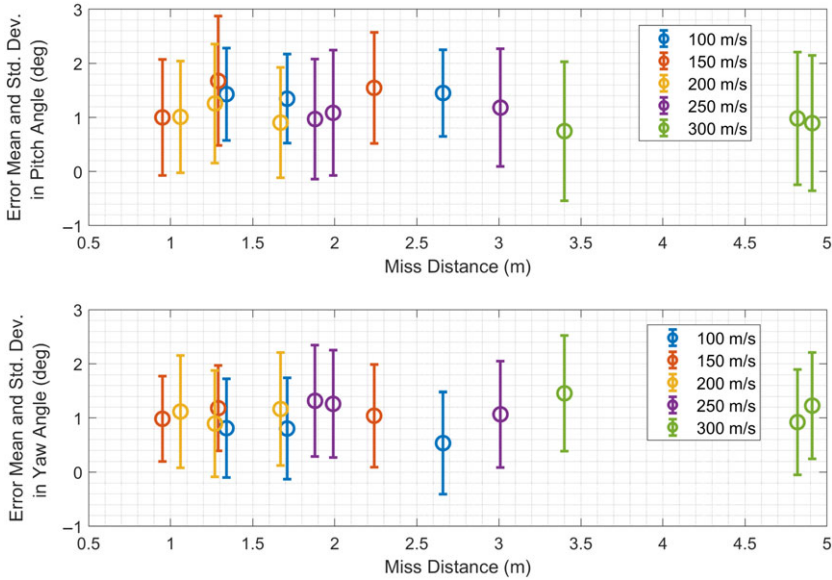
Figure 18. *The digital autopilot performance results for target manoeuvering at 2 g with different target speeds.*
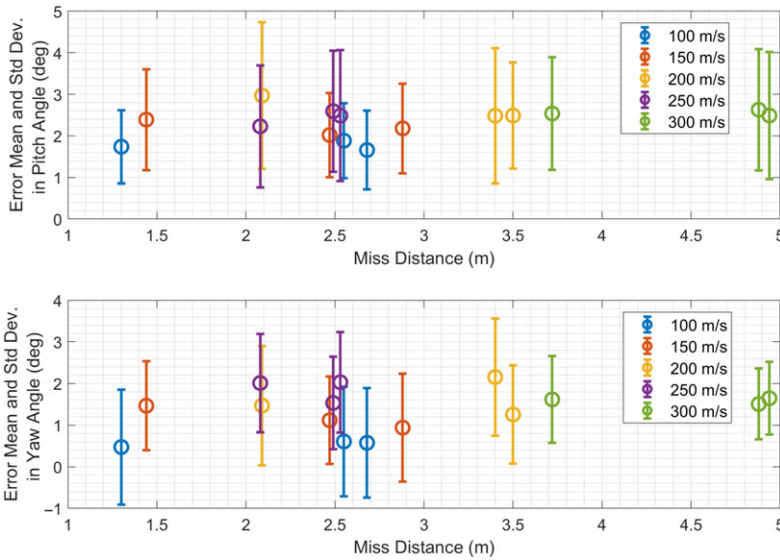
Figure 19. *The digital autopilot performance results for target manoeuvering at 3 g with different target speeds.*

5.0 Conclusion

Spinning missiles have complex dynamics compared to the roll-stabilised missiles. Couplings due to the rolling motion are so dominant, especially if the spinning rate is high (above 5 Hz). In terms of control, a single channel actuator with symmetric fins is enough to guide the missile in both pitch and yaw motion. However, this causes additional coupling effects if actuator and sensor delays and noise are significant. Old type spinning missile mostly use an analog (ON-OFF type) control approach that deflects fins to the minimum and maximum positions, and the control is achieved by applying phase shift between the minimum and maximum fin deflections during the roll cycle. This type of controller

requires precise roll angle measurements and fast actuator dynamics to work properly. In this work, a novel digital control approach is proposed to work on large actuator delays and sensor noise. In this approach, control signal shapes are predetermined in the design considering the decoupled dynamics. Instead of applying a phase shift, predetermined control signal shapes are applied, and the control is achieved by adjusting the amplitude of the signal at the beginning of each roll cycle based on the error dynamics. During a complete roll cycle, both the control signal amplitude and shape is fixed so that precise roll angle measurements or actuator delays are not effecting the performance significantly. The drawback of the digital controller is the requirement for a variable fin actuator system that is more complex and costly compared to the analog type ON-OFF actuator system.

To test the effectiveness of the controller, a detailed simulation environment, which covers the entire flight regime of a spinning missile, is generated. The aerodynamic model is generated by obtaining the static and dynamic coefficients via Missile DATCOM. The propulsion dynamics is based on the fuel mass and desired velocity profile of the missile. Systematic simulations are performed to test the performance of the proposed digital controller, and to compare with the conventional analog control approach. Results show that the digital controller works properly and gives significantly better performance compared to the analog approach under the influence of delays and noise caused by the actuator and sensor dynamics. As a future work, the digital and analog control approaches can be combined to design a hybrid control approach that might have more superior performance characteristics. Moreover, an integral term might be added to the digital controller to improve robustness against modeling errors.

References

[1] Zhou, W., Yang, S. and Dong, J. Coning motion instability of spinning missiles induced by hinge moment, *Aerospace Sci. Technol.*, 2013, **30**, (1), pp 239–245.

[2] He, S., Lin, D. and Wang, J. Coning motion stability of spinning missiles with strapdown seekers, *Aeronaut. J.*, 2016, **120**, (1232), pp 1566–1577.

[3] Fleeman, E.L. *Tactical Missile Design*, 2nd ed, American Institute of Aeronautics and Astronautics, 2006, *Reston*, Virginia, US.

[4] Nobahari, H. and Mohammadkarimi, H. Multiple-input describing function technique applied to design a single channel ON-OFF controller for a spinning flight vehicle, *Proc. Inst. Mech. Eng. G J. Aerospace Eng.*, 2012, 226, (6), pp 631–645.

[5] Chow, J., Chiesa., J., Dreyer, P., Eisman, M., Karasik, T.W, Kvitky, J. and Shirley, C. Protecting commercial aviation against the shoulder-fired missile threat, Rand Corp Santa Monica CA. No RAND/OP-106, 2005.

[6] Creagh, M.A. and Mae, D.J. Attitude guidance for spinning vehicle with independent pitch and yaw control, *J. Guidance Control Dyn.*, 2010, *33*, (3), pp 915–922.

[7] Li, K., Yang, S. and Zhao, L. Stability of spinning missiles with an acceleration autopilot, *J. Guidance Control Dyn.*, 2012, **35**, (3), pp 774–786.

[8] Yan, X., Yang, S. and Xiong, F. Stability limits of spinning missiles with attitude autopilot, *J. Guidance Control Dyn.*, 2011, **34**, (1), pp 278–283.

[9] Li, K., Yang, S. and Zhao, L. Three loop autopilot of spinning missiles, *Proc. Inst. Mech. Eng. G J. Aerospace Eng.*, 2014, 228, (7), pp 1195–1201.

[10] Yan, X., Yang, S. and Zhang, C. Coning motion of spinning missiles induced by the rate loop, *J. Guidance Control Dyn.*, 2010, 33, (5), pp 1490–1499.

[11] Fresconi, F., Cooper., G., Celmins, I., DeSpirito, J. and Costello, M. Flight mechanics of a novel guided spin-stabilised projectile concept, *Proc. Inst. Mech. Eng. G J. Aerospace Eng.*, 2012, **226**, (3), pp 327–340.

[12] Christopher, R., Joshua, D., Lamar, A., Mark, U. and William, B.B. Missile DATCOM User's Manual-2011 Revision, Army Aviation and Missile Research Development Eng Ctr Redstone Arsenal al System Simulation and Development Directorate, 2011.

[13] Zipfel, P.H. *Modeling and Simulation of Aerospace Vehicle Dynamics*, 2nd ed, American Institute of Aeronautics and Astronautics, 2007, *Reston*, Virginia, US.

[14] Stevens, B.L., Lewis, F.L. and Johnson, E.N. *Aircraft Control and Simulation: Dynamics, Controls Design, and Autonomous Systems*, 3rd ed, John Wiley & Sons, 2016.

[15] Elko, E.C., Howard, J.W., Kochanski, R.C., Nguyen, T.P.T. and Sanders, W.M. Rolling airframe missile: development, test, evaluation, and integration, *Johns Hopkins APL Tech. Dig.*, 2001, **22**, (4), pp 573–582.